colloids and interfaces

MDPI

Communication

On the *ac* Measurements of the Electrical Conductivity of Dilute Colloidal Electrolytes

Ioulia Chikina [1], Sawako Nakamae [2] and Andrey Varlamov [3,*]

[1] LIONS, NIMBE, CEA, CNRS, Université Paris-Saclay, CEA Saclay, 91191 Gif-sur-Yvette, France; julia.chikina@cea.fr
[2] Service de Physique de l'etat Condensé, SPEC, CEA, CNRS, Université Paris-Saclay, CEA Saclay, 91191 Gif-sur-Yvette, France; sawako.nakamae@cea.fr
[3] CNR-SPIN, Via del Fosso del Cavaliere, 100, 00133 Rome, Italy
* Correspondence: andrey.varlamov@spin.cnr.it

Abstract: The details of *ac*-conductivity measurements in a colloidal electrolyte cell with flat control gate electrodes are discussed. The use of impedance diagnostics in studies of transport phenomena in such systems requires caution in the definition of the thickness of the screening accumulation layers that appear along the metal-electrolyte interfaces. The value of this characteristic length λ_0 critically depends on the volume fraction $\phi_\odot$ of colloidal particles in the bulk of the electrolyte. Accounting for the dependence $\lambda_0(\phi_\odot)$ makes it possible to consistently explain the large discrepancy in the available experimental data regarding the influence of the colloidal fraction on the effective conductivity of the colloidal suspension.

Keywords: electrolytes; colloids; impedance measurements; accumulation layer

check for updates

Citation: Chikina, I.; Nakamae, S.; Varlamov, A. On the *ac* Measurements of the Electrical Conductivity of Dilute Colloidal Electrolytes. *Colloids Interfaces* **2023**, *7*, 58. https://doi.org/10.3390/colloids7030058

Academic Editor: Reinhard Miller

Received: 10 July 2023
Revised: 21 August 2023
Accepted: 10 September 2023
Published: 12 September 2023

1. Introduction

When describing the conductivity of a suspension of various stabilized solutions, in particular, when studying transport phenomena in dilute colloidal electrolytes (suspension of colloidal particles) containing magnetic nanoparticles, Maxwell's theory [1–3], which has long become a classic, is successfully used. The formula proposed by the latter for the conductivity of an inhomogeneous medium, consisting of a matrix with a conductivity σ_0, containing randomly located spherical inclusions with a conductivity of $\sigma_\odot$, has the form:

$$\frac{\sigma(\phi)}{\sigma_0} = 1 + \frac{3(\sigma_\odot/\sigma_0 - 1)\phi}{\sigma_\odot/\sigma_0 + 2 - (\sigma_\odot/\sigma_0 - 1)\phi}, \tag{1}$$

where ϕ is the relative volume occupied by the inclusions. In the case of inclusions which conductivity exceeds that one of the solvent, one can easily see that Maxwell's formula demonstrates the linear growth of effective conductivity $\sigma(\phi)$ in the region of weak concentrations ($\phi \ll 1$) with its saturation as ϕ grows in the case of $\sigma_\odot/\sigma_0 \gg 1$.

The application of Maxwell's formula to dilute colloidal electrolytes requires caution. Being immersed (or synthesized within) in the electrolyte solution, the colloidal particles of the bare radius R_0 acquire surface ions (e.g., hydroxyl groups, citrate, etc., [4–6] resulting in a very large structural charge eZ ($|Z| \gg 10$). Its sign can be both positive and negative, depending on the surface group type. The latter, in return, attracts counterions from the surrounding solvent creating an electrostatic screening coat of the size of the Debye length λ_0 with an effective charge $-eZ$. In these conditions, nano-particles approaching between them to the distances $r \leq \lambda_0$ begin to repel each other without floculation [7–9]. The region of an essential interaction between them corresponds to the condition

$$n_\odot^{(c)}(\lambda_0 + R_0)^3 \sim 1, \tag{2}$$

where $n_\odot$ is the density of colloidal particles, and superscript c indicates its critical value. In order for the electrolyte to remain homogeneous, it is necessary to avoid the overlapping of screening shells surrounding the core of the colloidal particles, that is, to limit ourselves to concentrations that satisfy the condition of applicability of the theory of Deryagin–Landau–Verwey–Overbeek [7–9]:

$$n_\odot(\lambda_0 + R_0)^3 \ll 1. \tag{3}$$

When Equation (1) is applied to a colloidal suspension, the dimensionless parameter of the theory $\phi \equiv \phi_\odot$ has to be identified namely with this quantity:

$$\phi_\odot \longleftrightarrow n_\odot(R_0 + \lambda_0)^3 \ll 1, \tag{4}$$

and, hence, only the linear regime in the concentration dependence of conductivity turns out to be available.

The characteristic features of the experimental works [10–13], where the Maxwell theory was used for the description of the obtained results, are the following:

- The validity of Equation (1) implicitly requires the uniformity (lack of dispersion) of individual characteristics of inclusions. The methods of preparation of dilute colloidal electrolytes containing maghemite nanoparticles in Refs. [10–13] allow the monitoring of the quality of this component with good accuracy and the control of the fulfillment of the requirement $\phi_\odot \ll 1$. This is a qualitative difference of the studies [10–13] from most of the transport experiments with the suspensions prepared mechanically (see, for example, reviews [14,15]).
- In all experiments of Ref. [10–15], the linear change of conductivity versus relative volume occupied by the inclusions is observed in the region $\phi \ll 1$. This characteristic feature gives grounds to use the Maxwell theory in the interpretation of the transport properties of various suspensions (see Figure 1 (taken from Ref. [12]) and the corresponding caption).

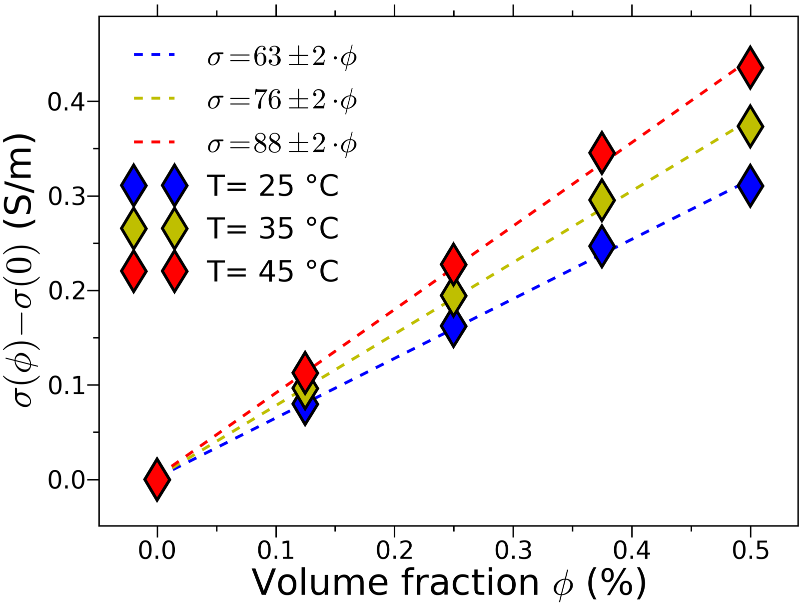

Figure 1. Conductivity of aqueous solution of colloidal maghemite particles as a function of their volume fraction at different temperatures [12]. The dashed lines are linear fits to the data with fitting parameters as indicated in the legend. The slopes of all these lines satisfy the requirement $(\sigma(\phi) - \sigma_0)/\sigma_0 \leq 3\phi$, following the analysis of formula (1) in the limit $\phi \ll 1$ and $\sigma_\odot \to \infty$. Taking into account that $\sigma_0 \approx 0.312\, S/m$, one can make sure that the data presented in this figure fulfill this requirement, which allows us to treat them within the Maxwell model.

Yet, it is necessary to attract attention to the fact that, in the most of such successful linear fittings of the observed $\sigma(\phi)$, the slope of this dependence dramatically exceeds that of the one allowed by the Maxwell theory. Indeed, the maximal slope $\sigma_0^{-1}\frac{d\sigma(\phi)}{d\phi}$ of the linear approximation of Equation (1) is reached when $\sigma_\odot \gg \sigma_0$ and it is equal to 3, while in the measurements of different years for mechanically prepared suspensions, it exceeds this theoretical limit by three orders: for example, in suspension aluminum/water, this value reaches 3.68×10^3 [16]. This is an overwhelming inconsistency which indicates the inapplicability of Maxwell's formalism to explain the cited experiments.

The lack of consistency is also deepened by the available data for obviously dielectric suspensions (see Ref. [17]). Namely, the conductivity $\sigma_\odot$ of coats in SiO nanoparticles (fumed silica) in ethylene glycol is less than the conductivity of the alcohol (SiO nanoparticles are good dielectrics). As a consequence, the expected effect of such powder inclusions on the conductivity of ethylene, where it is added, should be negative. Yet, as we see, the corresponding effect is positive (see Figure 2).

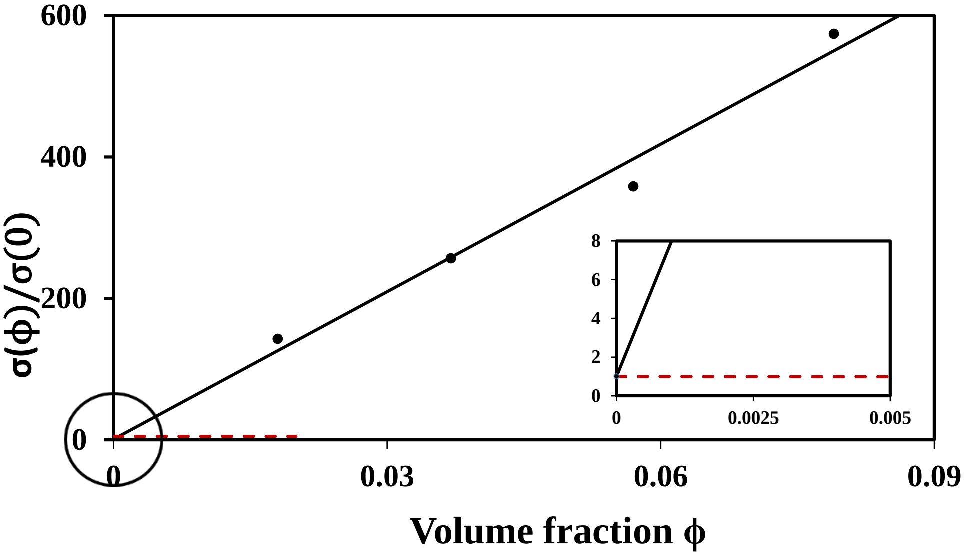

Figure 2. Growth of electrical conductivity of aluminium nitride-ethylene glycol nanofluid at 298.15 K [17]. Black dots represent the result of measurements; dashed line represents the prediction of the linear Maxwell theory $\sigma(\phi)/\sigma_0 = 1 - 3\phi/2$ (see Equation (1) with $\sigma_\odot = 0$). The solid line is the fitting of experimental results according to the formula $\sigma(\phi)/\sigma_0 = 1 + 6950.56\phi$. For better visibility, the relative positions of the solid line and the dashed line in the vicinity of the origin, indicated by a circle, are shown in the inset. The latter allows better recognition of the striking divergence between the observed values of conductivity and its predictions based on the immediate application of the Maxwell formula.

A similar situation takes place in suspensions containing nanotubes. Namely, in aqueous suspension of nanotubes [18] an increase in the conductivity of the suspension is observed, although carbon nanotubes are wide-gap semiconductors. At room temperature, their conductive properties are similar to those of classical dielectrics; hence, the influence of such additives on the effective conductivity of the suspension should be negative.

In this relation, let us stress the striking difference in conductivity values σ_0 in experiments with mechanical suspensions [16,17] and electrolytes containing magnetic nanoparticles [12]. Thus, in the paper [17], conductivity $\sigma_0 \simeq 0.43\,\mu\text{S/cm}$, while in the case of electrolytes [12], this value turns out to be four orders greater: $\sigma_0 \simeq 3 \times 10^3\,\mu\text{S/cm}$.

- An important "mark of distinction" which illustrates the applicability of the Maxwell theory to the suspension of stabilized solutions is the non-linearity of $\sigma(\phi_\odot)$ in the region $\phi_\odot \leq 1$. According to Refs. [1–3], the behavior of $\sigma(\phi_\odot)$ in this region loses its linearity, demonstrating the systematic deviation of the observed values of conductivity above the linear increase. At the same time, the data of Ref. [10] demonstrate the reverse trend in this region: the conductivity at high enough concentrations $\sigma(\phi_\odot)$ deviates below the linear asymptotic. The reasons of this discrepancy require special attention and will be discussed below (see Section 2).
- Ionic liquids. The paper [13] reported the structural and transport properties of the dilute solutions of maghemite nanoparticles in ionic liquids *Ethylammonium nitrate*. To elucidate the role of the solvent (water or ionic liquid) in the properties of dilute electrolytes, it is useful to compare what happens with maghemite nanoparticles in ionic liquids and aqueous stabilizing electrolytes.

The details of the corresponding discussion are presented in Section 3.

2. *ac* Impedance Diagnostics

Impedance ac (alternative current) diagnostics are regularly involved in the study of transport phenomena in conductive media. A common reason for resorting to ac-complications against the background of relatively simple methodological possibilities in the dc-mode (direct current mode) is the desire to exclude the influence on the IVC (current-volt characteristic) of contact phenomena accompanying dc measurements. In some cases (2d-electrons over helium), dc transport measurements are impossible by definition. In lightly doped semiconductors (dilute electrolytes), the situation is less critical, but problems with contact resistance persist (see [19,20]).

In the simplest case, impedance diagnostics deal with an RC circuit that obeys the equation [21]

$$R\frac{dQ(t)}{dt} + \frac{Q(t)}{C} = U(t), \tag{5}$$

where $Q(t)$ is the value of the charge of the electrodes at the moment t and $U(t) = U_0\cos(\omega t)$ is the ac-voltage applied to them. Other parameters: the resistance of the electrolyte filling the volume between the electrodes of a flat capacitor $R = L/[\sigma(\phi_\odot)S]$; the distance between them L; the conductivity of the electrolyte $\sigma(\phi_\odot)$ is taken in the form corresponding to the linear approximation of Maxwell's formula (1); the area of the electrodes S; the capacitance of a flat capacitor composed of plates C are time independent. Usually in electrical engineering, the resistor and the capacitor are considered as two separate elements of the circuit [22]. Let us stress that in the problem under consideration, both these values characterize the same cuvette. The specifics of its capacitance C is the essence of the present analysis and it will be discussed in detail below.

The corresponding current $J(t)$ generated in the cell is equal to

$$J(t) = \frac{U_0\cos(\omega t - \theta)}{\sqrt{R^2 + (\omega C)^{-2}}}. \tag{6}$$

The lock-in tester is capable of simultaneously measuring both real and imaginary parts of the impedance. In result, it provides information about the phase shift θ between the current $J(t)$ and the voltage $U(t)$:

$$\tan\theta(\omega) = -1/(\omega RC). \tag{7}$$

By measuring the dependence of $\theta(\omega)$ the value of the RC product can be extracted. Assuming the capacitance C to be known, one determines the resistance R.

In "real" liquid electrolytes and in charged colloidal solutions, however, the measured complex impedance contains contributions such as the leakage resistance, slow diffusions (related to the micro-structure of the electrodes, and/or large ions and particles), in addition to the constant phase element, which refers to the ion motions within the Debye length (electronic double layer) at the electrode/liquid interface. Consequently, Equation (6) cannot fully describe such multi-electrochemical phenomena, and it is customary to use more phenomenological models such as the Havriiliak–Negami model [23].

When the measurements are performed at such high frequencies that the phase shift becomes negligible, one can use an alternative of the RC measurement. Namely, let us follow the method of complex impedance and formally assume that the complex harmonic signal $\tilde{U}(t) = U_0 \exp(i\omega t)$ is applied to the cuvette filled by the electrolyte. Looking at Equation (5) with such "driving force", on the right-hand-side, one can easily see that after some relaxation period, the stationary oscillations of the"complex charge" (which can be considered as the integral of the complex current) $Q(t) = Q_0(\omega)\exp(i\omega t)$ will set in the system. The amplitude $Q_0(\omega)$ itself is the complex function of frequency and properties of the circuit, reflecting the existence of the retard of the charge oscillations at the capacitor plates with respect to the voltage applied. The corresponding imaginary part

$$\Im Q_0(\omega) = -CU_0 \frac{\omega\tau_0}{1+\omega^2\tau_0^2} \tag{8}$$

with $\tau_0 = RC$, as the characterization of the inertial properties of the circuit time constant, demonstrates the maximum at the frequency $\omega_{max} = 1/RC$.

Here, it is necessary to recall that we are interested in the dependence of the electrolyte resistance in the function of the nanoparticles concentration in it. Hence, to be consistent in the use of Equation (7), one has to also take into account the effect of the nanoparticles' presence on the capacity of the cuvette. When the role of capacitor plays the cell filled by pure water, the electric field penetrates between plates only at the distances of the order of the Debye length λ_0, which is much less than the distance between electrodes L ($\lambda_0 \ll L$) [8]:

$$C_0 \simeq \epsilon S/(8\pi\lambda_0). \tag{9}$$

Thus, the effective capacity turns out to be much larger than expected $\sim S/L$.

Turning to a well conducting suspension, i.e., either metallic or DLVO type inclusions of the radius R_0 in water ($L \gg R_0 \gg \lambda_0$), one creates the ground for the intensive adsorption of colloids at the metal–electrolyte interface (this effect was studied in detail in Ref. [24]).

Indeed, as the concentration of colloidal particles in the bulk of the electrolyte increases, their number in the vicinity of the electrode also grows, and, accordingly, the number of associated mirror images increases. Thus, an increasingly dense dipole gas of colloidal particles with corresponding images is formed in the vicinity of the electrode (see Figure 3).

Regarding a few words about properties of suspensions containing dielectric inclusions, for which $\sigma_{\odot} \to 0$, as follows from the general formula (1) and specially noted in the caption to Figure 2, such clusters reduce the effective conductivity of the suspension. However, in the case of impedance measurements, suspensions containing dielectric inclusions may demonstrate well-conducting properties (see data from Figure 2 in comparison with those of Figure 1). This is due to the interaction of dielectric nanoparticles with the metal–electrolyte interface, during which the latter behave similarly to DLVO-colloids, i.e., are attracted to the interface. Indeed, dielectric nanoparticles have a dielectric constant $\epsilon_d < \epsilon_{aq}$. As a consequence, their interaction with water ions surrounding each of the nanoparticles has the character of repulsion (see [21]). For as long as the nanoparticle is in the volume of the electrolyte, these forces, acting on it from different sides, mutually compensate each other. Near the interface, however, such compensation is violated, and the nanoparticle is "pressed" to the metal by the forces acting on it from the side of the liquid volume.

The described process (see details in Ref. [24]) is nothing but the adsorption of such colloidal particles, which can dramatically change the value of cell capacitance. In fact, the presence of each adsorbed colloid results in the cutting of a "hole" of area πa^2 at the metal boundary (see Figure 3, where such areas are shown as light circles in the contact zone of each colloid with its mirror image).

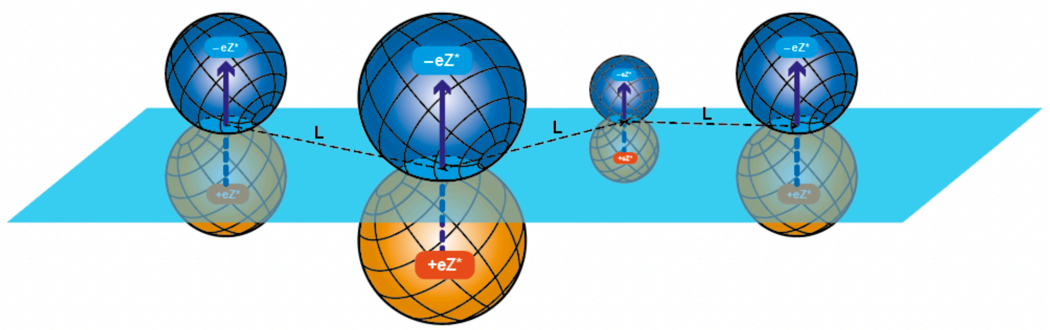

Figure 3. The gas of dipoles formed by the colloidal particles close to the metallic surface. The particles partially lost their coats. The average distance between the dipoles is $L \sim N_\odot^{-1/2}$, where $N_\odot$ is the surface concentration of the colloidal particles in the vicinity of the electrode. The light circles in the contact zone of each colloid with its mirror image have the radius $a = \sqrt{2\lambda_0 R_0 + \lambda_0^2}$.

In result, the value of capacitance C of the cell filled by water containing the DLVO inclusions considerably reduces, with respect to that one of the cell filled by pure water:

$$C = C_0 \frac{\lambda_0}{\lambda_\odot}, \quad \frac{1}{\lambda_\odot} = \frac{1}{\lambda_0}\left(1 - \pi a^2 N_\odot\right), \tag{10}$$

where $N_\odot$ is the density of adsorbed colloids. It was demonstrated (see Ref. [24]) that the latter is exponentially related to the volume one $n_\odot$ by means of the colloid's binding energy $E_\odot$:

$$N_\odot = n_\odot(R_0 + \lambda_0)\exp\left(\frac{|E_\odot|}{k_B T}\right), \tag{11}$$

where

$$E_\odot = -\frac{e^2 Z^2}{32\epsilon R_0}\frac{(3R_0 + 2\lambda_0)^2\lambda_0^2}{[3R_0^2 + 3R_0\lambda_0 + \lambda_0^2]^2}. \tag{12}$$

Let us see how the discussed-above peculiarities of the colloidal solution affect the procedure of measuring its conductivity:

$$\tan\theta(\omega) = -1/(\omega R C) = -\frac{4\pi\sigma(\phi_\odot)\lambda_\odot(\phi_\odot)}{\omega L}. \tag{13}$$

The area S is no longer included in this expression, but the cell length L remains, since the electrolytic capacity does not depend on it.

The idea of the above story is obvious. A standard instrument for measuring the conductivity of electrolytes is tuned to the specifics of contactless measurements of the ac-conductivity of charged liquids. The algorithm for the processing of the experimental information of this device does not contain information concerning the ability of the capacitor in the RC-chain to abrupt changes when the density of the suspension varies in the region of its small values. As a consequence, the measured phase shift $\theta(\omega)$ is controlled by the product $\sigma(\phi_\odot)\lambda_\odot(\phi_\odot)$, where the suspension's conductivity $\sigma(\phi_\odot)$ is determined by the Maxwell relation (1).

As we have demonstrated above, the screening length $\lambda_\odot$ (see Equation (11)) starts its exponential growth already at so small volume fractions such as $\phi_\odot \geq \exp\left(-\frac{|E_\odot|}{k_B T}\right)$. Since the values $\sigma(\phi_\odot)$ and $\lambda(\phi_\odot)$ enter in Equation (10) in the form of the product, one, analyzing the experimental data, can formally attribute the exponential growth of the thickness of the accumulation layer to that one of conductivity.

Note that the details of the description of experiments in the cited papers [10–15] devoted to measurements of the conductivity of suspensions of different types of nanoparticles are almost identical. Thus, the type of the used device is indicated, sometimes the operating frequency at which this device works optimally, and the results of the $\sigma(\phi_\odot)$ measurements are given, including the value of σ_0. All authors assume that the algorithms required to extract the dependence of $\sigma(\phi_\odot)$ from the impedance formalism are already included in the instrument software. However, as we have shown above, this is not the case when measuring the transport characteristics of nanoparticles' suspensions.

It is necessary to evaluate beforehand which situation we are talking about based on the behavior of the function $(\sigma(\phi_\odot) - \sigma_0)/\sigma_0$. If this value remains less than $3\phi_\odot$ for all investigated concentrations, as it is the case for the data presented in Figure 1, then the instrument together with its standard software can be trusted. If, however, when working with oxides (read, dielectrics), we, instead of $(\sigma(\phi_\odot) - \sigma_0)/\sigma_0 \approx -3\phi_\odot/2$, obtain an inversion of this combination by sign and $(\sigma(\phi_\odot) - \sigma_0)/\sigma_0 \gg \phi_\odot$ (as it takes place in Figure 2), the interpretation of the data using only Maxwell's formula (1) becomes meaningless.

In this case for the treatment of the data presented in Figure 2 using Equation (13), the product $\sigma(\phi_\odot)\lambda(\phi_\odot)$ becomes essential. The first multiplier takes into account the decrease of the suspension conductivity with an increase of the volume fraction ($\phi_\odot$ of dielectric nanoparticles; the second considers the influence of the latter's adsorption on the metal–electrolyte interface (see Equations (10) and (11)) on the capacitance value (see Equation (9)).

The proposed treatment of the anomaly in the behavior of $(\sigma(\phi_\odot)/\sigma_0$ for aluminium nitride granules in alcohol suspension (see Figure 2) is only qualitative and probably not the only one. But no alternative to our proposal is seen in the hundreds of papers on the subject, collected in reviews [14,15].

3. The Applicability of the Maxwell Model for Ionic Liquid Dilute Suspension

The compressibility and conductivity of colloidal solutions in ionic liquids was studied in Ref. [13] and compared with the analogous characteristics of aqueous solutions of the same colloids (see also Refs. [10–12,25]).

The results for compressibility obtained in Refs. [12,25] suggest that colloids in dilute ionic liquids behave similarly to $DLVO$-clusters in aqueous solutions. For what concerns the behavior of conductivity $\sigma_{aq}(\phi_\odot)$ of dilute aqueous solutions [12] and that one of ionic liquids $\sigma_{il}(\phi_\odot)$ [13], one can easily notice qualitative differences. The former shows a well-defined linear increase versus colloidal concentration (see Figure 2), which corresponds to predictions of the Maxwell model (see Equation (1)), while the latter remains unchanged in the limits of the measurements' accuracy (see Figure 4).

To recognize the source of this discrepancy, let us recall that the conductivity measurements of ionic liquid doped by magnetic colloids were performed by means of the ac-impedance diagnostics. The measured phase shift (see Equation (6)) contains the product of two $\phi_\odot$-dependent characteristics of the electrolyte: $R(\phi_\odot)C(\phi_\odot)$. While $R(\phi_\odot)$ with the growth of a colloidal concentration increases ([13]), the cell capacity $C(\phi_\odot)$ decreases and the resulting slope $d\sigma_{il}(\phi_\odot)/d\phi_\odot$ may well be close to zero. Moreover, there are examples when the slope $d\sigma_{aq}(\phi_\odot)/d\phi_\odot \to 0$, even in aqueous solutions of magnetic colloids (see Figure 4a from [11]).

The consistent interpretation of the discussed discrepancy requires some additional information regarding the capacitive properties of the cell used at the metal–ion liquid interfaces. However, the observed difference in the data of Figures 2 and 4 does not give grounds to refuse the use of the Maxwell model in interpretation of the properties of the ionic liquids.

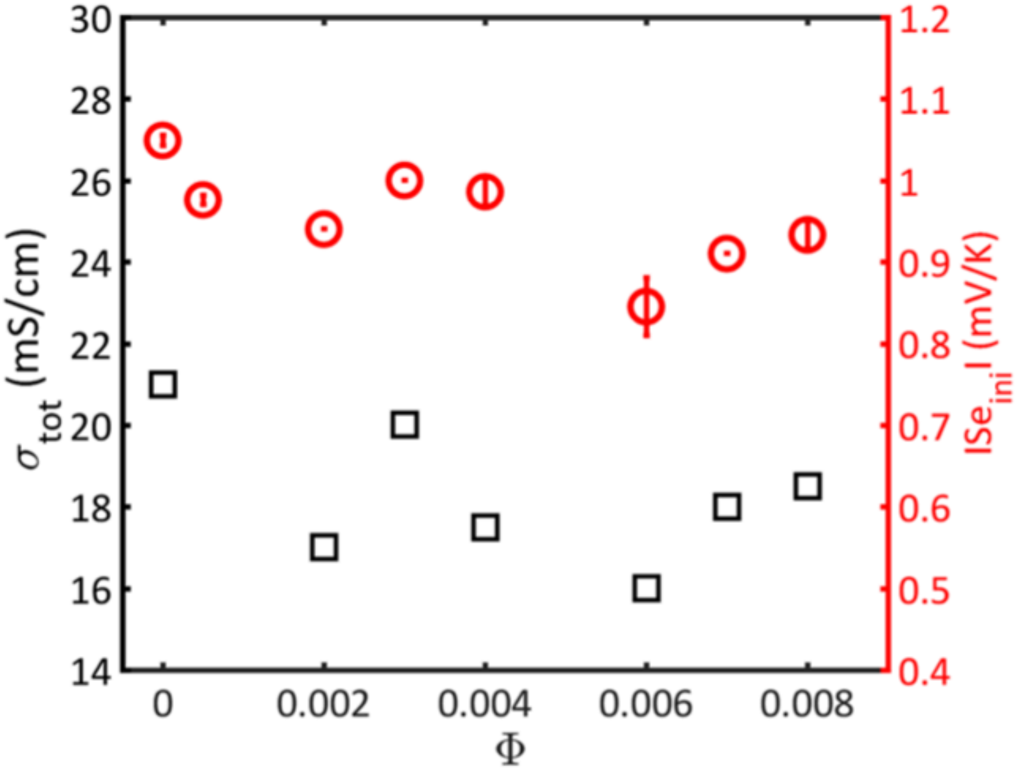

Figure 4. Conductivity of ionic-liquid suspension of maghnemite colloids depending on their volume fraction $\phi_{\odot}$ (taken from Ref. [13]). Ethylammonium Nitrate, mean cell temperature 25 °C (left side) ; Initial Seebeck effect $Se_{ini}(\phi_{\odot})$ in the same suspension (right side).

Among the bunch of colloidal solutions' conductivity measurements, the data of Ref. [13] take quite a worthy place, supplementing the existing variants of experiments with the actual scenario with ionic liquid as a conductive basis (along with pure water, its diluted solutions (acidic or alkaline), various alcohols, etc.)

It is useful to note that the data on the initial stage of the Seebeck effect for massive colloidal particles in an ionic liquid present in Figure 4 satisfactorily correlate with the behavior of conductivity $\sigma_{il}(\phi_{\odot})$ under the same conditions. This fact, noted in Ref. [26], confirms the general consistency of the proposed interpretation of the details of *ac*-transport in colloidal media based on the Maxwell model. The mechanisms of conductivity involving the Brownian motion, or aggregation phenomena, are less clear, especially in the linear ϕ domain.

4. Conclusions

The details of impedance diagnostics of conducting properties of a flat electrolyte cell filled with a dilute colloidal suspension were discussed. It is shown that, in the *RC*-model of such a cell, the capacitance *C* is determined by the effective thickness of the metal–electrolyte boundaries along which the screening accumulation layers are formed. This circumstance noticeably affects the measured imaginary part of the impedance of the cell with the electrolyte, allowing at least a qualitative explanation of the reasons for the systematic inconsistency of the Maxwell's theory (Equation (1)) predictions regarding the conductive properties of various liquid suspensions with experimental findings of Refs. [14,15].

It is necessary to point out that our consideration is performed in the quasi-stationary approximation, i.e., in the hypothesis that the accumulation layers succeed to follow the applied electromagnetic field. This assumption requires that the frequency of the measurements must be much less than the conductivity of the nano-particle counter-ions coats: $\omega \ll \sigma_{\odot}$, which is not too restrictive; for example, in experiment [12], the conductivity of the electrolyte $\sigma_0 \approx 0.312\,\mathrm{S/m}$ corresponds to the frequency 3 GHz. The condition imposed by the value of the nano-particle counter-ion coats' conductivity is even less restrictive since $\sigma_{\odot} \gg \sigma_0$. The account for the kinetics of the accumulation layer formation was undertaken in the review article [27].

We emphasize that the current boom in studies of the transport properties of nanoparticle suspensions is associated with hopes for their serious practical applications. A multiple increase in the conductivity (thermal conductivity) of a suspension by adding a small amount of suitable nanoparticles is a very attractive prospect in solving problems of heat removal, heat supply, in nuclear energy, etc. The result of our work appeals to make such statements more cautiously, having previously made sure that the observed anomalies in the transport properties of nanosuspensions do not have an "instrumental" origin.

Author Contributions: I.C.: Methodology, Formal analysis, Writing—review and editing, Visualization, Funding acquisition. S.N.: Analysis of experimental data, Writing—review and editing, Visualization, Funding acquisition. A.V.: Methodology, Formal analysis, Writing—review and editing, Visualization, Funding acquisition. All authors have read and agreed to the published version of the manuscript.

Funding: This research was supported by the European Union's Horizon 2020 Research and Innovation Programme: under grant agreement No.731976 (MAGENTA).

Data Availability Statement: Data sharing is not applicable to this article as no new data were created or analyzed in this study.

Acknowledgments: The authors are grateful to Valeriy Shikin, Emmanuelle Dubois, and Régine Perzynski for valuable discussions.

Conflicts of Interest: The authors declare no conflict of interest.

References

1. Maxwell, J. *A Treatise of Electricity and Magnetism*, 3rd ed., Oxford University Press: London, UK, 1892; Volume 1, part II. [CrossRef]
2. Fricke, H. A Mathematical Treatment of the Electric Conductivity and Capacity of Disperse Systems I. The Electric Conductivity of a S uspension of Homogeneous Spheroids. *Phys. Rev.* **1924**, *24*, 575–587. [CrossRef]
3. Bruggeman, D. Berechnung verschiedener physikalischer Konstanten von heterogenen Substanzen. I. Dielektrizitätskonstanten und Leitfähigkeiten der Mischkörper aus isotropen Substanzen. *Ann. Phys.* **1935**, *416*, 636–664. 4160705. [CrossRef]
4. Riedl, J.C.; Akhavan Kazemi, M.A.; Cousin, F.; Dubois, E.; Fantini, S.; Loïs, S.; Perzynski, R.; Peyre, V. Colloidal Dispersions of Oxide Nanoparticles in Ionic Liquids: Elucidating the Key Parameters. *Nanoscale Adv.* **2020**, *2*, 1560–1572. [CrossRef] [PubMed]
5. Bacri, J.C.; Perzynski, R.; Salin, D.; Cabuil, V.; Massart, R. Ionic ferrofluids: A crossing of chemistry and physics. *J. Magn. Magn. Mater.* **1990**, *85*, 27–32. [CrossRef]
6. Dubois, E.; Cabuil, V.; Boué, F.; Perzynski, R. Structural analogy between aqueous and oily magnetic fluids. *J. Chem. Phys.* **1999**, *111*, 7147–7160. [CrossRef]
7. Derjaguin, B.V.; Landau, L.D. Theory of the stability of strongly charged lyophobic sols and of the adhesion of strongly charged particles in solutions of electrolytes. *Acta Phys. Chem. URSS* **1941**, *14*, 633–662. [CrossRef]
8. Landau, L.D.; Lifshitz, E.M. *Statistical Physics (Course of Theoretical Physics)*, 3rd ed.; Elsevier: Amsterdam, The Netherlands, 2011; Volume 5, pp. 276–278.
9. Verwey, E.; Overbeek, J. *Theory of the Stability of Lyophobic Colloids*; Elsevier: Amsterdam, The Netherlands, 1948.
10. Lucas, I.; Durand-Vidal, S.; Bernard, O.; Dahirel, V.; Dubois, E.; Dufrêche, J.F.; Gourdin-Bertin, S.; Jardat, M.; Meriguet, G.; Roger, G. Influence of the volume fraction on the electrokinetic properties of maghemite nanoparticles in suspension. *Mol. Phys.* **2014**, *112*, 1463–1471. [CrossRef]
11. Salez, T.J.; Huang, B.T.; Rietjens, M.; Bonetti, M.; Wiertel-Gasquet, C.; Roger, M.; Filomeno, C.L.; Dubois, E.; Perzynski, R.; Nakamae, S. Can charged colloidal particles increase the thermoelectric energy conversion efficiency? *Phys. Chem. Chem. Phys.* **2017**, *19*, 9409–9416. [CrossRef] [PubMed]
12. Sani, E.; Martina, M.; Thomas, S.; Nakamae, S.; Dubois, E.; Peyre, V. Multifunctional Magnetic Nanocolloids for Hybrid Solar-Thermoelectric Energy Harvesting. *Nano. Mater.* **2021**, *11*, 1031. [CrossRef] [PubMed]
13. Bhattacharya, K.; Sarkar, M.; Salez, T.J.; Nakamae, S.; Demouchy, G.; Cousin, F.; Dubois, E.; Michot, L.; Perzynski, R.; Peyre, V. Structural, Thermodiffusive and Thermoelectric Properties of Maghemite Nanoparticles Dispersed in Ethylammonium Nitrate. *ChemEngineering* **2020**, *4*, 5. [CrossRef]
14. Minea, A. A Review on Electrical Conductivity of Nanoparticle-Enhanced Fluids. *Nano. Mater.* **2019**, *9*, 1592. [CrossRef] [PubMed]

15. Poongavanam, G.; Duraisamy, S.; Vigneswaran, V.S.; Ramalingam, V. Review on the electrical conductivity of nanofluids: Recent developments. *Mater. Today Proc.* **2021**, *39*, 1532–1537. [CrossRef]
16. Ganguly, S.; Sikdar, S.; Basu, S. Experimental investigation of the effective electrical conductivity of aluminum oxide nanofluids. *Powder Technol.* **2009**, *196*, 326–330. [CrossRef]
17. Zyla, G.; Vallejo, J.P.; Fal, J.; Lugo, L. Nanodiamonds–Ethylene Glycol nanofluids: Experimental investigation of fundamental physical properties. *Int. J. Heat Mass Transf.* **2018**, *121*, 1201–1213. [CrossRef]
18. Glover, B.; Whites, K.W.; Hong, H.; Mukherjee, A.; Billups, W.E. Effective electrical conductivity of functional single-wall carbon nanotubes in aqueous fluids. *Synth. Met.* **2008**, *158*, 506–508. [CrossRef]
19. Anselm, A. *Introduction to Semiconductor Theory*; Prentice-Hall: Hoboken, NJ, USA, 1981.
20. Robinson, R.; Stokes, R. *Electrolyte Solutions*; Butterworths Scientific Publications: London, UK, 1959.
21. Landau, L.D.; Lifshitz, E.M. *Electrodynamics of Continuous Media*; Elsevier: Amsterdam, The Netherlands, 2013.
22. Sommerfeld, A. *Electrodynamics (Lectures on Theoretical Physics)*; N.Y Academic Press Inc.: New York, NY, USA, 1952; Volume 3.
23. Havriliak, S.; et Negami, S. A complex plane representation of dielectric and mechanical relaxation processes in some polymers. *Polymer* **1967**, *8*, 161–210. [CrossRef]
24. Chikina, I.; Nakamae, S.; Shikin, V.; Varlamov, A. Charged colloids at the metal–electrolyte interface. *Colloids Interfaces* **2022**, *6*, 25. [CrossRef]
25. Gomes, R.; Ferreira da Silva, A.; Kouyaté, M.; Demouchy, G.; Mériguet, G.; Aquino, R.; Dubois, E.; Nakamae, S.; Roger, M.; Depeyrot, J.; et al. Thermodiffusion of repulsive charged nanoparticles—The interplay between single-particle and thermoelectric contributions. *Phys. Chem. Chem. Phys.* **2018**, *20*, 16402–16413. [CrossRef] [PubMed]
26. Chikina, I.; Nakamae, S.; Shikin, V.; Varlamov, A. Two-stage seebeck effect in charged colloidal suspensions. *Entropy* **2021**, *23*, 150. [CrossRef] [PubMed]
27. Chassagne, C.; Dubois, E.; Jiménez, M.L.; M van der Ploeg, J.P.; van Turnhout, J. Compensating for electrode polarization in dielectric spectroscopy studies of colloidal suspensions: Theoretical assessment of existing methods. *Front. Chem.* **2016**, *19*, 30. [CrossRef] [PubMed]